AD-A083 547 CORNELL UNIV ITHACA N Y DEPT OF THEORETICAL AND APP--ETC F/G 21/2
MATHEMATICAL THEORY OF LAMINAR COMBUSTION. IX. BURNER FLAMES.(U)
MAR 80 J D BUCKMASTER, G S LUDFORD DAAG29-79-C-0121
UNCLASSIFIED TR-111 ARO-15882.14-M NL

1 OF 1
AD A
083547

END
DATE
FILMED
5-80
DTIC

ARO 15882.14-M

ADA083547

LEVEL II

Department of
Theoretical and Applied Mechanics
CORNELL UNIVERSITY
ITHACA, NEW YORK

MATHEMATICAL THEORY OF LAMINAR COMBUSTION IX:

Burner Flames

Technical Report No. 111

J.D. Buckmaster & G.S.S. Ludford

March 1980

U.S. Army Research Office
Research Triangle Park, NC 27709

Contract No. DAAG29-79-C-0121

Cornell University
Ithaca, NY 14853

Foreward

This report is Chapter IX of the twelve in a forthcoming research monograph on the mathematical theory of laminar combustion. Chapters I-IV originally appeared as Technical Reports Nos. 77, 80, 82 & 85; these were later extensively revised and then issued as Technical Summary Reports No's 1803, 1818, 1819 & 1888 of the Mathematics Research Center, University Wisconsin-Madison. References to I-IV mean the MRC reports.

Contents

A

The findings of this report are not to be construed as an official Department of the Army position unless so designated by other authorized documents.

Chapter IX

Burner Flames

1. Features of an Anchored Flame.

A common enough observation, both inside and outside the laboratory, is that a premixed flame can be positioned stably at the mouth of a tube through which the mixture passes. Such a flame is usually conical (though not necessarily so), in which case it is conveniently divided into three parts: the tip, the base (near the rim of the tube) and the bulk of the flame in between. The latter gives it roughly the shape of a cone.

Elementary considerations of the flame speed and the nature of the flow adequately explain the conical shape (see Fig. VIII.2 and the accompanying discussion). Simple hydrodynamic considerations provide salient features of the associated flow field, as we shall see in Sec. 2.

The nature of the combustion field in the vicinity of the rim is crucial in questions of existence and stability of the flame. Gas speeds near the tube wall are small, because of viscous effects, so that if the flame could penetrate there it would be able to propagate against the flow, travelling down the tube in a phenomenon known as flashback. In point of fact, the flame is quenched at some distance from the wall, so as to prevent its reaching the low-speed region, the fundamental quenching mechanism (for a stationary flame) being heat loss by conduction to the tube. Such quenching enables unburnt gas to escape betweeen the flame and the wall through what is known as the dead space. A mathematical description of this phenomenon is presented in Sec. 5.

The heat loss to the tube also plays an important role in the global stability of the combustion field. If the flame is disturbed so that its

speed increases it will move closer to the rim, threatening flashback. But heat loss will then increase, causing a decrease in the temperature of the flame and hence its speed, so that it will be swept away again. Similarly, if there is a decrease in flame speed so that the flame is swept away from the rim, threatening so-called blowoff, heat conduction to the wall decreases, the speed increases and the flame moves back again. Thus heat loss acts as a restoring force.

The third part of a burner flame, the tip, is similar in one respect to the base in that here also the flame approaches a boundary, albeit an adiabatic one, namely the centerline. Experiment shows that the tip may be closed, the flame cutting the centerline at right angles, or open, the flame being quenched (though not by heat loss) at a finite distance from the centerline so as to leave a dead space or hole through which the mixture escapes unburnt (Fig. 1). Which of these two possibilities occurs depends on the composition of the mixture and flow conditions. Flame tips are treated in Secs. 3 & 4.

2. Hydrodynamic Considerations.

Consider a weak plane flame, of speed εU (with $0 < \varepsilon << 1$), lying stationary in an infinite uniform flow

(1) $$\underset{\sim}{v} = (U,0).$$

The hydrodynamic jump conditions (VIII.1,2,3) are satisfied by the undisturbed flow (1) ahead of the flame and

(2) $$\underset{\sim}{v} = (U, \pm\varepsilon U(\rho_1/\rho_2 - 1))$$

behind, where the sign is opposite to that of the slope of the flame. There is

simply a refraction of the streamlines, and we may expect that to be the primary characteristic of the flow field in the neighborhood of any point on the conical part of the burner flame. A more detailed description requires a hydrodynamic analysis, which we shall pursue some distance assuming that the flame speed is constant. Such an assumption is correct if the burner is sufficiently large; in the context of slowly varying flame the voluminal stretch in equation (VIII.43) is then small so that the burning rate $M_n = 1$.

We shall first look for a plane flame tip in which the uniform flows (1) and (2) hold far upstream; elsewhere it is necessary to solve Euler's equations on each side of the constant-speed flame. A Poisseuille distribution would be more realistic for the upstream flow ahead of the flame, but the analysis is much easier for a uniform flow while still uncovering the essential characteristics.

Although we are not necessarily dealing with a slowly varying flame, the notation ξ, η of Sec. VIII.3 will be used to emphasize that the distance unit is large compared to the flame thickness. The ξ-axis is now taken along the symmetry line (Fig. 2); velocity components are u, v. Since the flame slopes gently (in the main), we may write

$$(3) \qquad \eta = F(\sigma) \quad \text{with } \sigma = \varepsilon \xi$$

for its upper surface. In front u, p and $\partial/\partial\eta$ are $O(1)$ while v and $\partial/\partial\xi$ are $O(\varepsilon)$. The momentum equation therefore shows that p is a function of σ alone, to order ε, from which

$$(4) \qquad u = f(\sigma) + O(\varepsilon^2)$$

follows on applying Bernoulli's equation; continuously then requires

(5) $$v = -\varepsilon\eta f'(\sigma) + O(\varepsilon^2).$$

The condition for the flame to be at rest is

(6) $$fF = -U\sigma + O(\varepsilon^2)$$

when σ is measured from the tip.

The appropriate coordinates in the burnt gas are σ and

(7) $$\nu = \varepsilon\eta.$$

At the flame we have

(8) $$u_2 = f + O(\varepsilon^2),\ v_2 = \varepsilon(\rho_1 U/\rho_2 + fF') + O(\varepsilon^2)$$

according to the jump conditions while, on the centerline, symmetry requires

(9) $$v = 0 \quad \text{for} \quad \sigma > 0.$$

Since the flow is a perturbation of the uniform one upstream, we may write

(10) $$u = U + \varepsilon u' + O(\varepsilon^2),\ v = \varepsilon v' + O(\varepsilon^2),$$

which immediately implies

(11) $$f = U + O(\varepsilon) \quad \text{and hence} \quad F = -\sigma + O(\varepsilon).$$

The flame is wedge shaped and the boundary conditions (8) yield

(12) $$u_2' = 0,\ v_2' = U(\rho_1/\rho_2 - 1)$$

if the flow upstream is to be unperturbed.

Since the vorticity is constant on the undisturbed streamlines, the flow downstream is the superposition of a potential motion, satisfying the boundary conditions (9) and (12b), and a shear motion (with $v' = 0$) induced by the boundary conditions (12a). Thus

$$u' = \frac{U(\rho_1/\rho_2 - 1)}{\pi} \ln(\nu/\varepsilon r), \quad v' = \frac{U(\rho_1/\rho_2 - 1)}{\pi}\phi \tag{13}$$

where r, ϕ are polar coordinates corresponding to σ, ν. The flow field is sketched in Fig. 2. Note the singularity in u' for $\phi = 0$, which presumably implies that the flow differs significantly from uniform there. The nature of this wake has not been investigated, so that the description is incomplete at the present time.

A similar treatment is possible for axisymmetric flames; only the changes in the previous formulas need be mentioned. With η denoting distance from the axis of symmetry, the corresponding velocity component is

$$v = -\frac{1}{2}\varepsilon\eta f'(\sigma) + O(\varepsilon^2), \tag{14}$$

so that the flame is at rest if

$$fF' + \frac{1}{2}f'F = -U + O(\varepsilon^2). \tag{15}$$

Nevertheless the results (11) still hold, as do the boundary conditions (9) and (12). We now find

$$u' = 0, \quad v' = \frac{1}{2}\varepsilon\, U(\rho_1/\rho_2 - 1)\tan\phi/2, \tag{16}$$

showing that the disturbance is $o(\varepsilon)$ everywhere except near the cone $\phi = \pi - \varepsilon$ on which the flame lies. That is reflected in Fig. 3, where the

streamlines straighten out much faster than in Fig. 2; there is no wake. Note that the deflection of the streamlines at the flame is the same in the two cases, namely $\epsilon U(\rho_1/\rho_2 - 1)$.

The streamline tracing of actual flames (Fig. 1) differ in two respects. The flow ahead of the flame is not uniform but is essentially Poisseuille; and finite values of ϵ give rise to a pressure gradient which is associated with the divergence of the streamlines there.

3. Slowly Varying Flame Tips.

The question that we examine here is whether the equation (VIII.32) governing slowly varying flames admits solutions corresponding to the tips (Sivashinsky 1974, 1975). The difficulty of the hydrodynamic problem, even when the burning rate is prescribed (Sec. 2), leads us to sever the coupling with Euler's equations by setting

(17) $$\underset{\sim}{v}_1 = U(1,0,0),$$

in accordance with the constant-density approximation (Sec. I.5).

If ψ is the inclination of the flame, then

(18) $$M_n = \rho_1 U \sin\psi, \ v_{\perp 1} = U\cos\psi$$

so that, in the plane case (Fig. 4),

(19) $$\underset{\sim}{v}_{\perp 1}\cdot\underset{\sim}{\nabla}_{\perp} M_n = \rho_1 U^2\cos^2\psi\frac{d\psi}{ds}, \ \underset{\sim}{\nabla}_{\perp}\cdot\underset{\sim}{v}_{\perp 1} = -U\sin\psi\,\frac{d\psi}{ds}$$

and the governing equation becomes

(20) $$\frac{d\psi}{ds} = k\sin^3\psi\,\ell n\left(\frac{\sin\psi}{\sin\alpha}\right),$$

where

$$k = -2T_*^2\rho_1^2 U/b \quad \text{and} \quad \alpha = \operatorname{cosec}^{-1}\rho_1 U. \tag{21}$$

The implicit requirement $\rho_1 U > 1$ simply reflects the fact that a stationary flame can only exist in a flow that moves faster than the adiabatic flame speed. For comparison with the axially symmetric case to follow, it is more convenient to use η as independent variable, in terms of which the equation becomes

$$\frac{d\psi}{d\eta} = k \sin^2\psi \, \ell n\left(\frac{\sin\psi}{\sin\alpha}\right). \tag{22}$$

Apart from $\psi = \alpha$ and $\pi - \alpha$, only three integral curves are shown in Fig. 4a. The remainder can be found by horizontal translation. Those which lead to shapes with $\psi \to \alpha$ or $\pi - \alpha$ as $\xi \to -\infty$, as required, are shown in Figs. 4b,c. In Fig. 4b the curves 1 and 5 represent a family filling in the wedge between the straight lines 2 and 4. In Fig. 4c, only these lines are obtained.

For $\mathcal{L} > 1$ (i.e. $b < 0$ and $k > 0$) a smooth tip is possible, namely 3, and presumably that should be chosen over the whole family of cusped tips which are available. For $\mathcal{L} < 1$ (i.e. $b > 0$ and $k < 0$), no smooth tip is possible; only the wedge-shaped tip formed by 2 and 4 is offered by the theory.

Turning to the axisymmetric case, we find that equations (18) and (19a) still hold but that (19b) is replaced by

$$\nabla_\perp \cdot v_{\perp 1} = \frac{U}{\eta}\frac{d}{ds}(\eta\cos\psi) \tag{23}$$

because of the radial (η) divergence. Hence the governing equation now becomes

$$\frac{d\psi}{d\eta} - \frac{\sin\psi\cos\psi}{\eta} = k \sin^2\psi \, \ell n\left(\frac{\sin\psi}{\sin\alpha}\right), \tag{24}$$

with k and α defined as before, where η ranges over positive values only.

Because of the new term the integral curves, shown in Fig. 5a, no longer have the translation property, though they have the same shape as in the plane case as $\eta \to \infty$. Only those asymptoting $\phi = \pi - \alpha$ as $\eta \to \infty$ are acceptable, which leads to the open (including re-entrant) possibilities in Fig. 4b, as well as one closed, but only to the single open possibility in Fig. 4c. Representative curves are shown, as marked; all open curves approach the centerline as $\xi \to \pm\infty$.

For $\mathcal{L} > 1$ (i.e. $b < 0$ and $k > 0$) a closed tip is possible, namely 2, and presumably that occurs rather than either a re-entrant or open one. (Cf. later remarks concerning flame temperature.) For $\mathcal{L} < 1$ (i.e. $b > 0$ and $k < 0$) only one tip is available and that is open. In short, the theory of slowly varying flames predicts closed tips for $\mathcal{L} > 1$ and open tips for $\mathcal{L} < 1$. It is noteworthy that open tips are found experimentally (Lewis & von Elbe 1961, p. 309) for both lean hydrogen and rich heavy hydrocarbon mixtures. In each case the deficient component diffuses much more readily than the component in excess, and indeed calculations based on values given by Kanury (1977, pp. 385 et seq.) show that $\mathcal{L} = 0.23$ and 0.81, respectively, for mixtures with air.

The flame temperature is readily deduced from the formula (VIII.30) as

$$H_1 + 2\theta^{-1} H_1 \ln M_n = H_1 + 2\theta^{-1} H_1^2 \ln(\sin\psi/\sin\alpha). \tag{25}$$

In all cases the adiabatic flame temperature H_1 is approached, of course, as $\psi \to \pi - \alpha$ at large distances. When $\mathcal{L} > 1$, the temperature tends to a maximum

(26) $$H_1 + 2\theta^{-1}H_1^2 \ln \operatorname{cosec} \alpha$$

at the very tip, irrespective of whether the flame is plane or axisymmetric. On the other hand, when $\mathcal{L} < 1$ the temperature does not change along a plane tip but decreases like

(27) $$H_1 + 2\theta^{-1}H_1^2 \ln \psi$$

for an axisymmetric tip, giving an unbounded perturbation. (The same result holds for the open tips in Fig. 5b, so that the closed tip selected is the only one without this singularity.) Such unboundedness means that the temperature differs by more than $O(\theta^{-1})$ from the adiabatic value; so the asymptotic structure is not uniformly valid and a different kind of analysis is required. While such an analysis has not yet been attempted, the drop in temperature suggests that the flame is extinguished; so that the profile of Fig. 4c should be truncated at some large value of ξ, giving a flame more in accord with experimentally observed open tips. For the plane tip, non-uniformity manifests itself geometrically rather than through a singularity in the flame temperature: the pointed tip violates the assumption of slow variation on which the analysis is based.

The dramatic change in the nature of the solution as $\mathcal{L}$ passes through 1, together with the breakdown of the analysis of $\mathcal{L} - 1 = O(\theta^{-1})$, suggests that flame tips should be investigated when the diffusion of heat is almost the same as that of the reactant, i.e. under the near-equidiffusional assumption. That has been done by Buckmaster (1979b), whose work is the subject of the next section.

4. Near-Equidiffusional Flame Tips.

The general formulation of near-equidiffusional flames as elliptic free-boundary problems is given in Sec. VIII.5. Moreover, if the constant-density approximation is invoked to uncouple the fluid mechanics and the flame is immersed in a uniform flow whose speed is much greater than the flame speed, then these problems reduce to ones of Stefan type (as is shown in Sec. VIII.6).

To describe flame tips, take the χ-axis along the centerline. For upstream the flame is either wedge shaped or conical with half-angle $\pi/4$, corresponding to the adiabatic value 1 for the flame speed. Only $y > 0$ is considered, because of symmetry in the plane case and by definition in the axially symmetric. Take

$$y = F(\chi) \tag{28}$$

as the locus of the flame, choosing the origin of χ sufficiently far upstream for $F(0)$ to be large. Near $\chi = 0$ the combustion field is that of a plane flame, so that equations (III.13,14) hold with $\mathcal{L} = 1 + \lambda/\theta$ and x measured vertically down, i.e. on $\chi = 0$ we have

$$T = T_1 + Y_1 e^{y-F(0)}, \quad h = \lambda Y_1[F(0) - y]e^{y-F(0)} \quad \text{for} \quad 0 < y < F(0), \tag{29}$$

$$T = T_* = H_1, \; h = 0 \quad \text{for} \quad y > F(0), \tag{30}$$

which will be taken as initial conditions. Stricly speaking, these conditions are valid only in the limit $F(0) \to \infty$ but, because the exponential can be made arbitrarily small near $y = 0$, any desired accuracy can be obtained by taking $F(0)$ sufficiently large.

The equations to be solved are

$$(31)\quad \partial T/\partial\chi = \mathbb{L}_\nu(T),\ \partial h/\partial\chi = \mathbb{L}_\nu(h+\lambda T) \quad \text{for} \quad 0 < y < F(\chi),$$

$$(32)\quad T = T_* = H_1,\ \partial h/\partial\chi = \mathbb{L}_\nu(h) \quad \text{for} \quad y > F(\chi)$$

(cf. Sec. III.6), where

$$(33)\quad \mathbb{L}_\nu \equiv \frac{1}{y^\nu}\frac{\partial}{\partial y}\, y^\nu \frac{\partial}{\partial y}$$

and $\nu = 0$ or 1 according as the flame is plane or axisymmetric. The accompanying jump conditions are

$$(34)\quad [\partial h/\partial y] = -\lambda[\partial T/\partial y] = \lambda Y_1 \exp(h_*/2T_*^2) \quad \text{at} \quad y = F(\chi),$$

T and h being continuous there. To these we must add the symmetry conditions

$$(35)\quad \partial T/\partial y = \partial h/\partial y = 0 \quad \text{at} \quad y = 0$$

and, finally,

$$(36)\quad h \to 0 \quad \text{as} \quad y \to \infty ,$$

consistent with the formula (30).

At first glance it seems questionable that the present formulation, based as it is on the assumption that the gas speed is much greater than the flame speed, could provide an adequate description of flame tips. Indeed at a smooth closed tip the two speeds are equal on the centerline. But there is no such difficulty for open tips; if the flame speed is small in the far field, we may expect it to remain small everywhere so that uniformly valid results are obtained. Our analysis could therefore lead to open-tip solutions

only, whatever the parameter values. In fact it also generates closed-tip solutions, albeit ones that are not valid near the centerline. Since the unit of length is the preheat thickness (at $\chi = 0$), the region of non-uniformity is extremely small.

The analysis is completed by numerical integration which for such parabolic systems involves marching downstream, i.e. the direction of the time-like variable χ. Both plane and axisymmetric flames have been computed by Buckmaster (1979), for $T_1 = 0.2$, $Y_1 = 1.0$ and several values of λ. He also computed the limit solution as $\lambda \rightarrow -\infty$ in each case, to which we shall come shortly.

Results for plane flames are shown in Fig. 6. Note that there is no appreciable curvature until F has decreased to about 3, at least for $\lambda < 10$. Then the cold fringe of the pre-heat zone reaches the centerline and interaction with the conditions (35) begins, the effect of the interaction depending on λ. For non-negative values the speed of the flame increases monotonically, bending it around towards the centerline, which it intersects at right angles. Apparently the tip is smooth with F proportional to $(\chi_0 - \chi)^{1/2}$ near the intersection point χ_0, a conclusion that is supported by a similarity solution there for $\lambda = 0$ (Buckmaster 1979a). These values of λ give $\mathcal{L} > 1$, when smooth closed tips were also found for slowly varying flames. Moreover, as λ increases above 10 the flame begins to curve at progressively larger values of F, as if it were trying to get onto the scale of the slowly varying flame.

For small enough negative values of λ the flame still closes smoothly although its speed initially decreases, resulting in a somewhat extruded tip. For larger negative values the flame speed decreases to zero at the point

labelled Q where the curve has a horizontal tangent. The curve for $\lambda = -50$ typifies this behavior, which is shown in extreme form for $\lambda = -\infty$.

The limiting curve as $\lambda \to -\infty$ can be obtained as follows. Assume that h is $O(\lambda)$ for $0 < y < F(\chi)$ but remain $O(1)$ for $y > F(\chi)$, as is suggested by the initial conditions (29). Then the function

$$(37) \qquad \hat{h} = h/\lambda$$

is identically zero for $y > F(\chi)$, i.e. outside the tip, and we need only solve the simpler problem

$$(38) \qquad \frac{\partial T}{\partial \chi} = L_\nu(T), \ \frac{\partial \hat{h}}{\partial \chi} = L_\nu(\hat{h}+T) \text{ for } 0 < y < F(\chi),$$

$$(39) \qquad T = T_1 + Y_1 e^{y-F(0)}, \ \hat{h} = Y_1[F(0)-y]e^{y-F(0)} \text{ at } \chi = 0 \text{ for } 0 < y < F(0),$$

$$(40) \qquad T = H_1, \ \hat{h} = 0, \ \partial(T + \hat{h})/\partial y = 0 \text{ at } y = F(\chi),$$

$$(41) \qquad \partial T/\partial y = \partial \hat{h}/\partial y = 0 \text{ at } y = 0$$

inside the tip.

The perturbation temperature h_* tends to follow the changes in flame speed. It has a finite negative value at Q, showing once more that curved flames cannot necessarily be treated as locally plane (when h_* would tend to $-\infty$). The numerical integration can be continued downstream from Q without difficulty, the profile first curving away from the centerline and then back to it to form a closed tip. There is no experimental evidence for such a bulbous tip and indeed having burnt mixture ahead of the flame, as would be the case just past Q, would certainly need justification. Our first-order analysis of the flame sheet does not distinguish between the

two sides: there are no convection terms in equations (VIII.55). It is conceivable that at the next order, which does take account of convection, there is no acceptable structure. Such would be a sound mathematical reason for rejecting the solution beyond $\chi = \chi_Q$.

Buckmaster proposes to terminate the solutions at χ_Q, so that Q is thereby identified with quenching. Downstream there is no chemical reaction, the unburnt gas below Q simply mixing with the burnt gas above. That is, the values of T and h on $\chi = \chi_Q$ are used as initial conditions for a smooth solution of the parabolic equations (31), which now hold for all values of y. Such a reactionless solution is consistent in that T immediately drops below H_1, the temperature at which reaction occurs: while the initial temperature for $y > F(\chi_Q)$ is equal to H_1, that for $0 < y < F(\chi_Q)$ is less. Agreement with slowly varying flames for $\mathcal{L} < 1$ can be obtained by supposing that the wedge shape found there is actually open at the vertex.

The axisymmetric results (Fig. 7) are qualitatively similar, but there is one sharp quanititative difference. Azimuthal curvature affects the flame speed (through the terms in $y^{-1}\partial/\partial y$) long before the pre-heat zone reaches the centerline. As a consequence, the flame starts to curve much further from the centerline (at about $F = 40$) than for the plane flame. (Figs. 6 & 7 should be compared.) Likewise the dead space between Q and the centerline is more than five times larger. In short, open plane tips are much narrower than their axisymmetric counterparts, a result also found for slowly varying flames with $\mathcal{L} < 1$ if the wedge is supposed to be open on the present scale. A similar comparison holds for $\mathcal{L} > 1$, so that the present analysis provides a smooth transition from the general characteristics of slowly varying flames for $\mathcal{L} < 1$ to those for $\mathcal{L} > 1$.

A word of caution is needed. The transition from a closed to an open tip occurs for large negative values of λ, between -20 and -50 for a plane flame and -50 and -100 for an axisymmetric one. Since λ/θ is assumed small, the result will probably be quantitatively meaningful only for large values of the activation energy θ, values so large as to be seldom (if ever) realized in practice.

5. Quenching by a Cold Surface.

A crucial role in the existence and stability of a burner flame is played by quenching near its base, as we have already remarked in Sec. 1. However, the situation near the rim of a burner is complicated, involving not only heat transfer but also a multi-dimensional flow field with mixing between the reactants and the cold ambient atmosphere. To throw some light on the phenomenon of quenching by a cold wall, the present section will examine a simple model (Buckmaster 1979a) which, admittedly, discards much that is relevant to the combusion field near a burner rim. Since heat transfer by conduction plays the central role in the phenomenon, near-equidiffusional flames provide an appropriate framework.

Consider a parallel flow of combustible gas moving over the plane $y = 0$ with a velocity U_y. A linear shear flow is the simplest representative of realistic flows near the surface, but any other could be handled just as easily (Buckmaster also considers a uniform flow.) Located in the flow is a stationary premixed flame (Fig. 8), which is influenced by the presence of the wall as a diffusion inhibitor and heat sink.

The flame locus is again described by equation (28) with the origin of chosen to make $F(0)$ large. Far upstream, where the flame is uninfluenced

by the wall, it still propagates with unit velocity but now into a flow with speed $UF(\chi)$. Consequently it follows the parabola

$$F = [F^2(0) - 2\chi]^{1/2}, \tag{42}$$

though this fact does not change the initial conditions (29, 30) but is solely a check on the subsequent computations.

In focussing on the effect of heat loss we shall, for simplicity, take $\lambda = 0$. In the limit $U \to \infty$ the equations with which we have to deal are

$$y\partial(T,h)/\partial\chi = L_0(T,h) \quad \text{for} \quad 0 < y < F(\chi), \tag{43}$$

$$T = T_* = H_1, \; y\partial h/\partial\chi = \mathbb{L}_0(h) \quad \text{for} \quad y > F(\chi), \tag{44}$$

these being the modifications of equations (31,32) which take account of the shear flow. The accompanying jump conditions are

$$[\partial T/\partial y] = -Y_1 \exp(h_*/2T_*^2), \; [\partial h/\partial y] = 0 \quad \text{at} \quad y = F(\chi) \tag{45}$$

while T and h are continuous there. The condition (36) still holds, of course.

Finally we come to conditions at the wall. The heat flux there is assumed small in order to avoid excessive variations in the flame temperature (cf. Sec. VIII.2); specifically

$$\partial T/\partial y = k(T - T_1)/\theta \;\text{at}\; y = 0 \tag{46}$$

to all orders, where k is a prescribed positive constant and T_1 is, as before, the temperature of the fresh mixture. Such a condition is appropriate for a thin, poorly conducting wall whose other surface is maintained at the

temperature T_1. Otherwise it may be considered an assumption which avoids coupling the temperature field in the wall with that in the flow without compromising the essential physics. We shall also take the wall to be chemically inactive, i.e.

(47) $$\partial Y/\partial y = 0 \quad \text{at} \quad y = 0$$

to all orders. The boundary conditions are therefore

(48) $$\partial T/\partial y = 0, \ \partial h/\partial y = k(T - T_1) \quad \text{at} \quad y = 0.$$

The main simplification for $\lambda = 0$ is that h can be removed from the problem. Thus $y\partial h/\partial \chi = \mathbb{L}_0(h)$ everywhere and h has no discontinuities at the flame sheet, so that it can be written explicitly in terms of its normal derivative at the wall and hence, according to the condition (48), the surface temperature. At the flame sheet it becomes

$$h_* \ k \ \frac{3^{1/6}\Gamma(1/3)}{2\pi} \int_{-\infty}^{\chi} \frac{[T_1 - T(s,0)]}{(\chi - s)^{3/2}} \exp[-\frac{1}{9}\frac{F^3(\chi)}{\chi - s}]ds,$$

which then determines the temperature gradient (45) on the cold side of the flame in terms of the surface temperature up to that station. We are left with a (numerical) problem for T and F alone.

Results are shown in Fig. 8 for various values of the heat-loss parameter k. The flame sheet intersects the wall at right angles when k is small, F being proportional to $(\chi_0 - \chi)^{1/3}$ near the intersection point χ_0 (as Buckmaster shows by a similarity solution there). Exactly what happens very close to the wall cannot be revealed by our analysis, since the assumption of a large flow speed (which reduces the elliptic problem to a parabolic one) is

not valid when y is small. A reasonable conclusion from the failure of the heat loss to generate a dead space on the scale of the flame thickness is that flashback occurs.

When k is large enough ($\geq 7 \cdot 2\pi/3^{1/6}\Gamma(1/3)$ is sufficient) the flame sheet becomes horizontal at some point Q, which is identified with quenching as in Sec. 4. (Again the numerical solution can be continued beyond Q until ultimately the flame sheet intersects the wall.) Failure to adopt such a hypothesis in the present context would lead to the unexpected conclusion that $O(\theta^{-1})$ heat loss is incapable of quenching a flame. We therefore propose that the region between Q and the wall is a deadspace through which unburnt mixture can pass downstream, the generation of such a gap being the mechanism by which heat loss prevents flashback. The conclusion is in sharp contrast with that for a plane flame (Sec. III.4), for which extinction occurs when the loss is sufficient to reduce the flame speed to $e^{-1/2}$.

REFERENCES

Buckmaster, J. 1976, The quenching of deflagration curves, Combust. Flame 26, 151-162.

Buckmaster, J. 1979a, The quenching of two-dimensional premixed flames, Acta Astronaut. (to appear).

Buckmaster, J. 1979b, A mathematical description of open and closed flame tips, Combust. Sci. Tech. (to appear).

Kanury, A.M. 1975, Introduction to Combustion Phenomena, New York: Gordon & Breach.

Lewis, B. & von Elbe, G. 1961, Combustion, Flames & Explosions of Gases. New York: Academic Press.

Sivashinsky, G.I. 1974, The diffusion stratification effect in bunsen flames, J. Heat Transfer (Trans. ASME), 11, 530 - 535.

Sivashinsky, G.I. 1975, Structure of Bunsen flames, J. Chem. Phys. 62, 638-643.

Fig. 1 Closed and open flame tips (Lewis & von Elbe Figs. 109 & 150.)

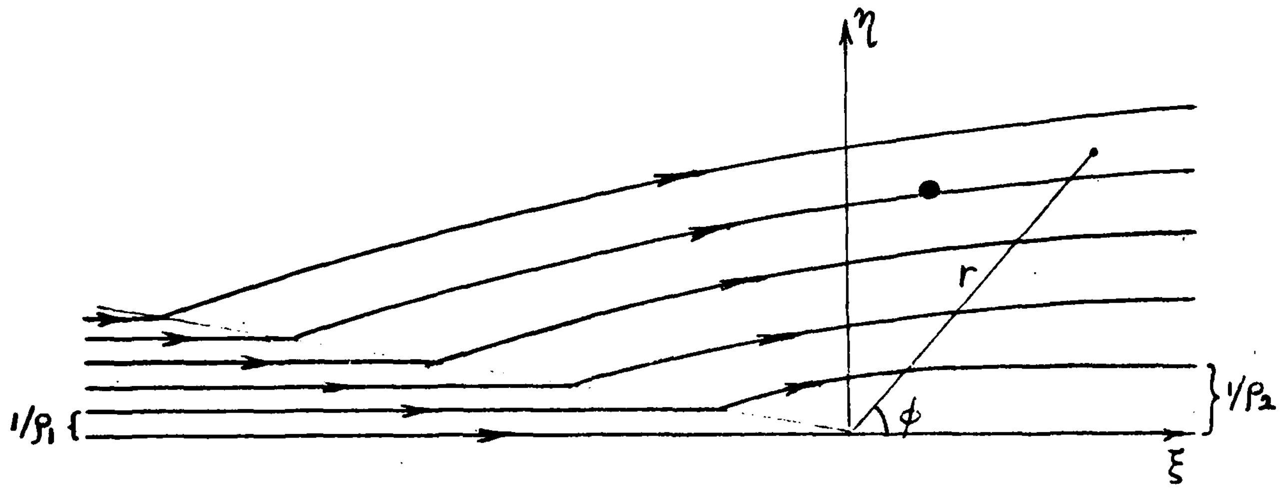

Fig. 2 Plane tip for constant flame speed. Drawn for
$\epsilon(\rho_1/\rho_2 - 1)/\pi = 0.1$, $\epsilon = \tan^{-1} 10°$.

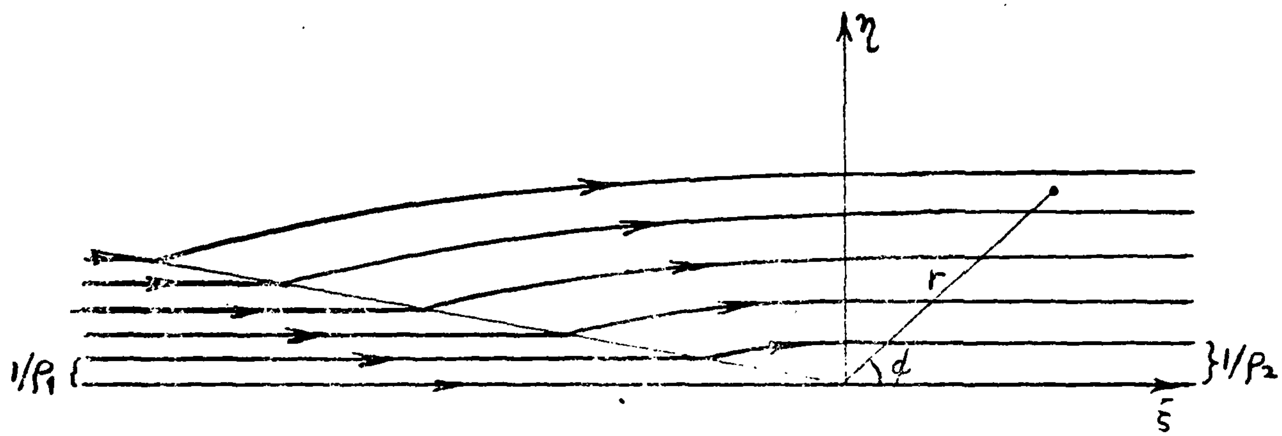

Fig. 3 Axisymmetric tip for constant flame speed. Same parameter values as Fig. 2.

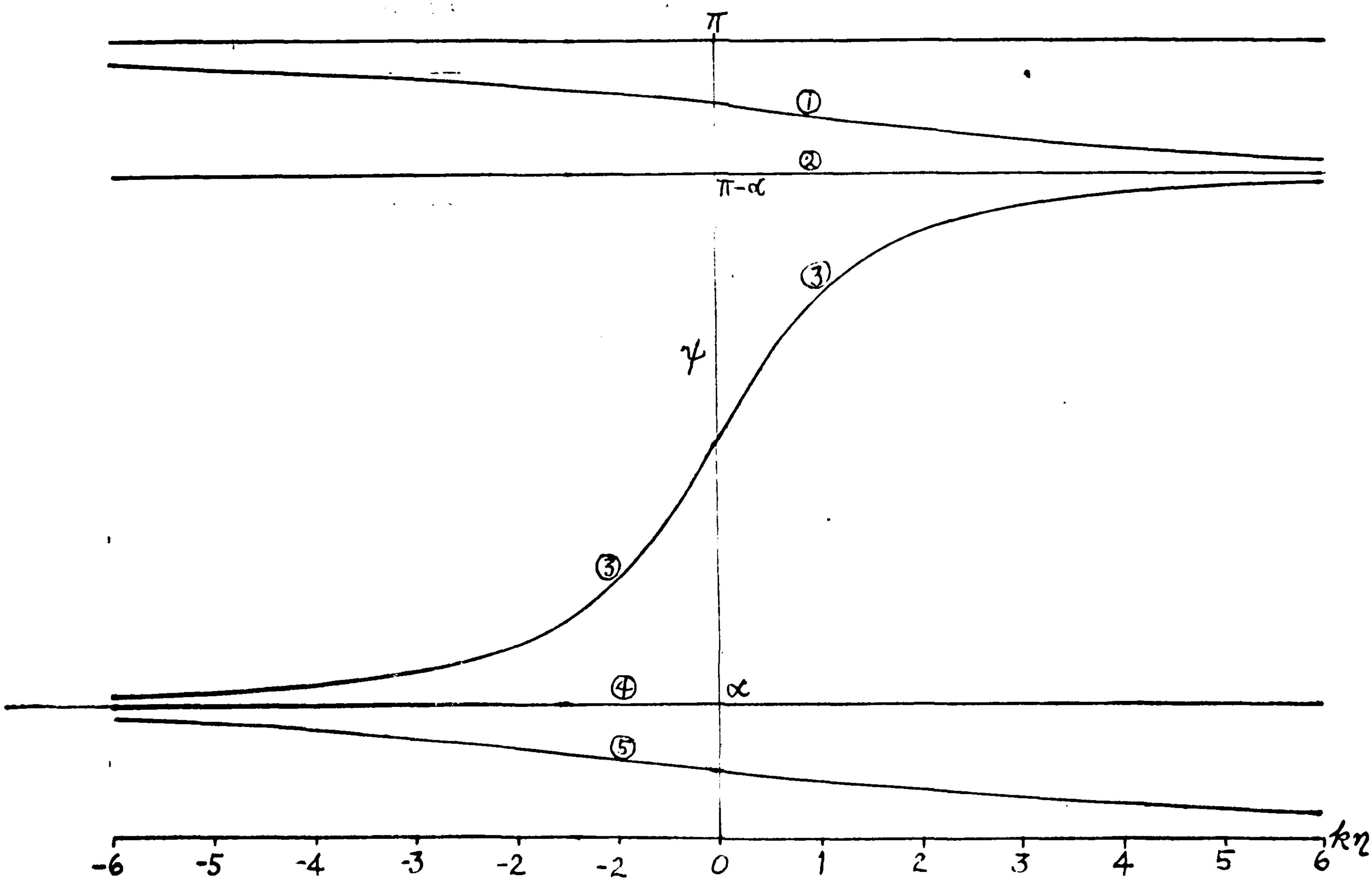

Fig. 4 Slowly varying plane tips, drawn for $\alpha = \pi/6$ and $k = \pm 1$.
(a) Integral curves of equation (22).

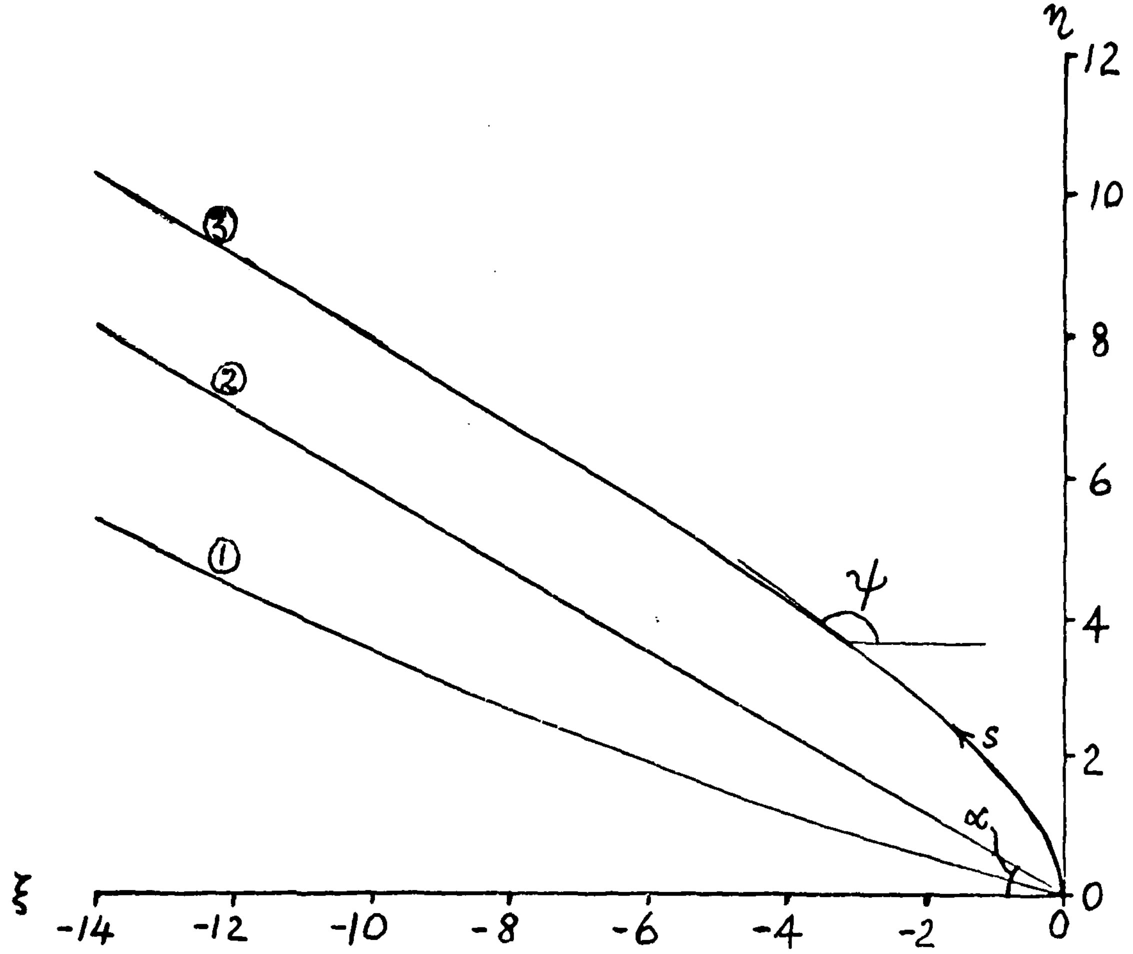

Fig. 4 (b) Possible shapes when $\mathcal{L} > 1$ $(k > 0)$.

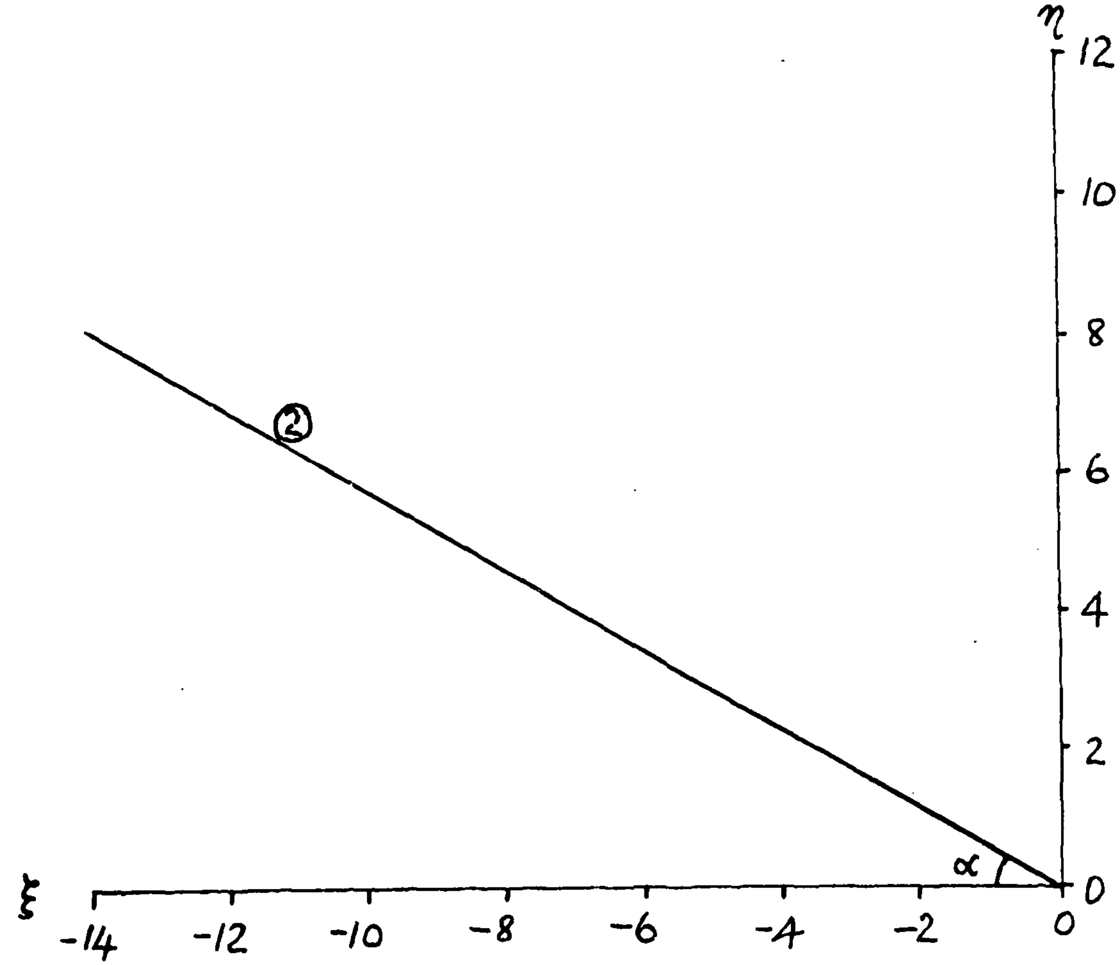

Fig. 4(c) Only possible shape for $\mathcal{L}<1$ $(k<0)$.

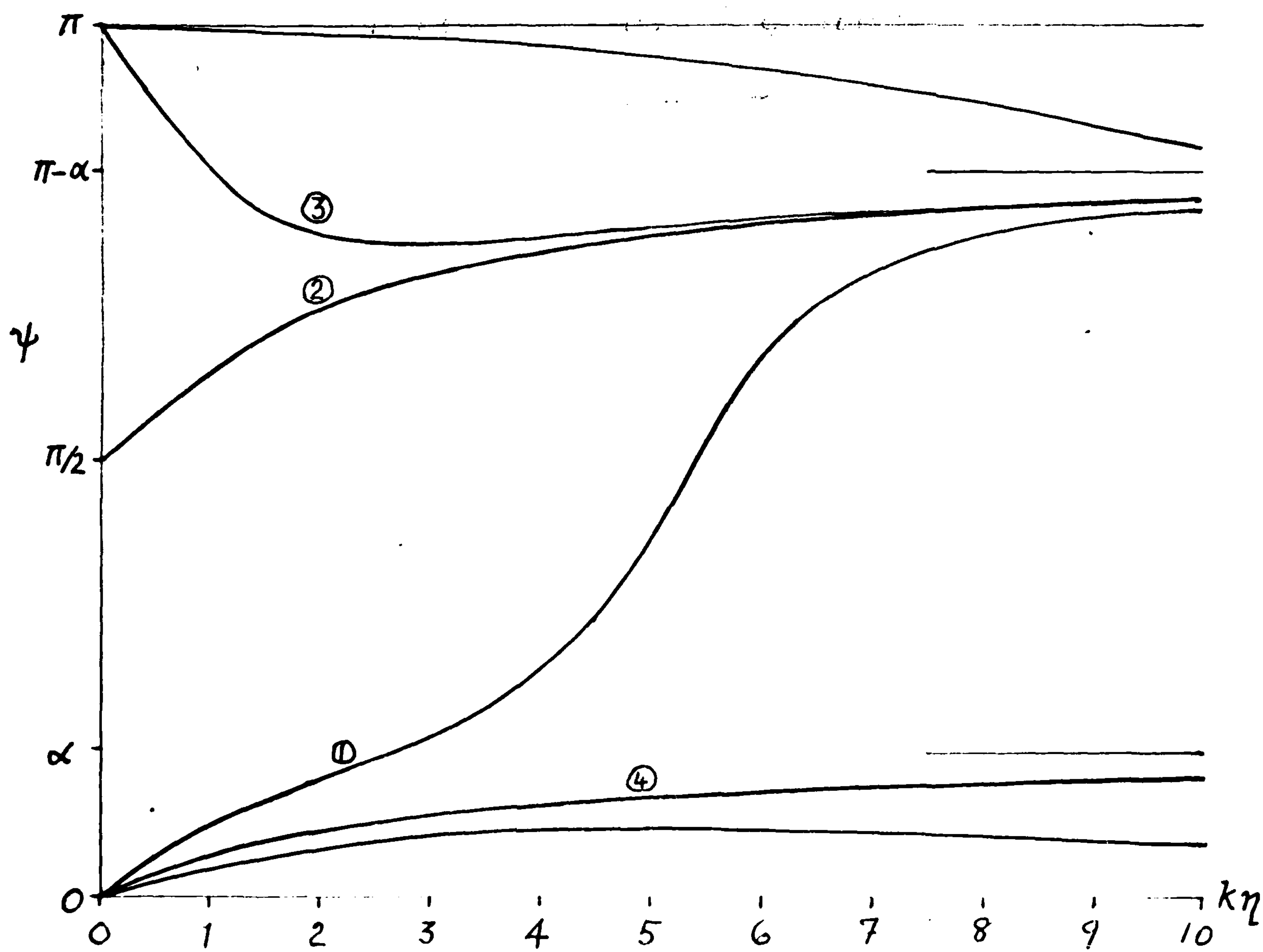

Fig 5 Slowly varying axisymmetric tips, drawn for $\alpha = \pi/6$ and $k = \pm 1$.
(a) Integral curves of equation (24). for $k = +1$.

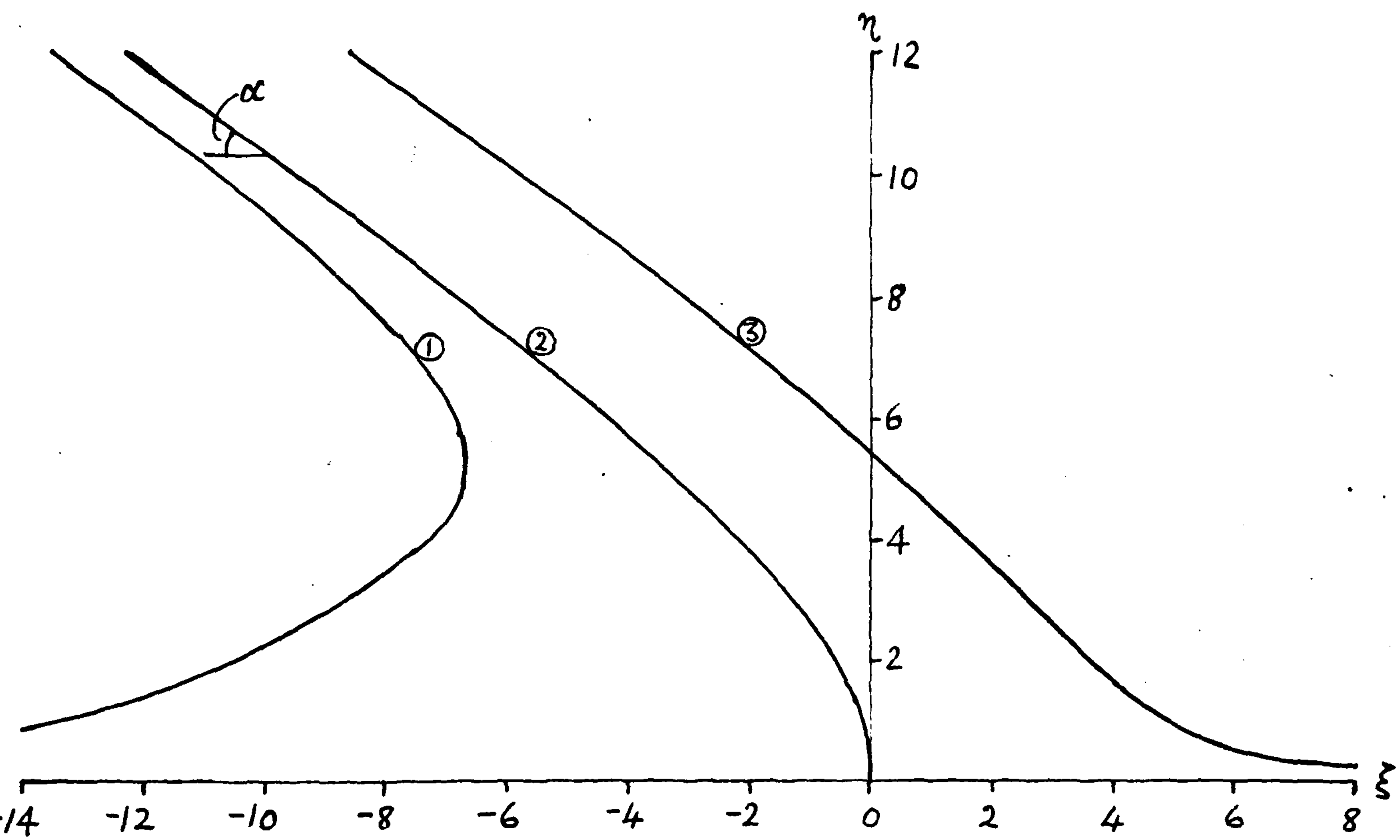

Fig. 5(b) Possible shapes for $\mathcal{L}>1$ $(k>0)$.

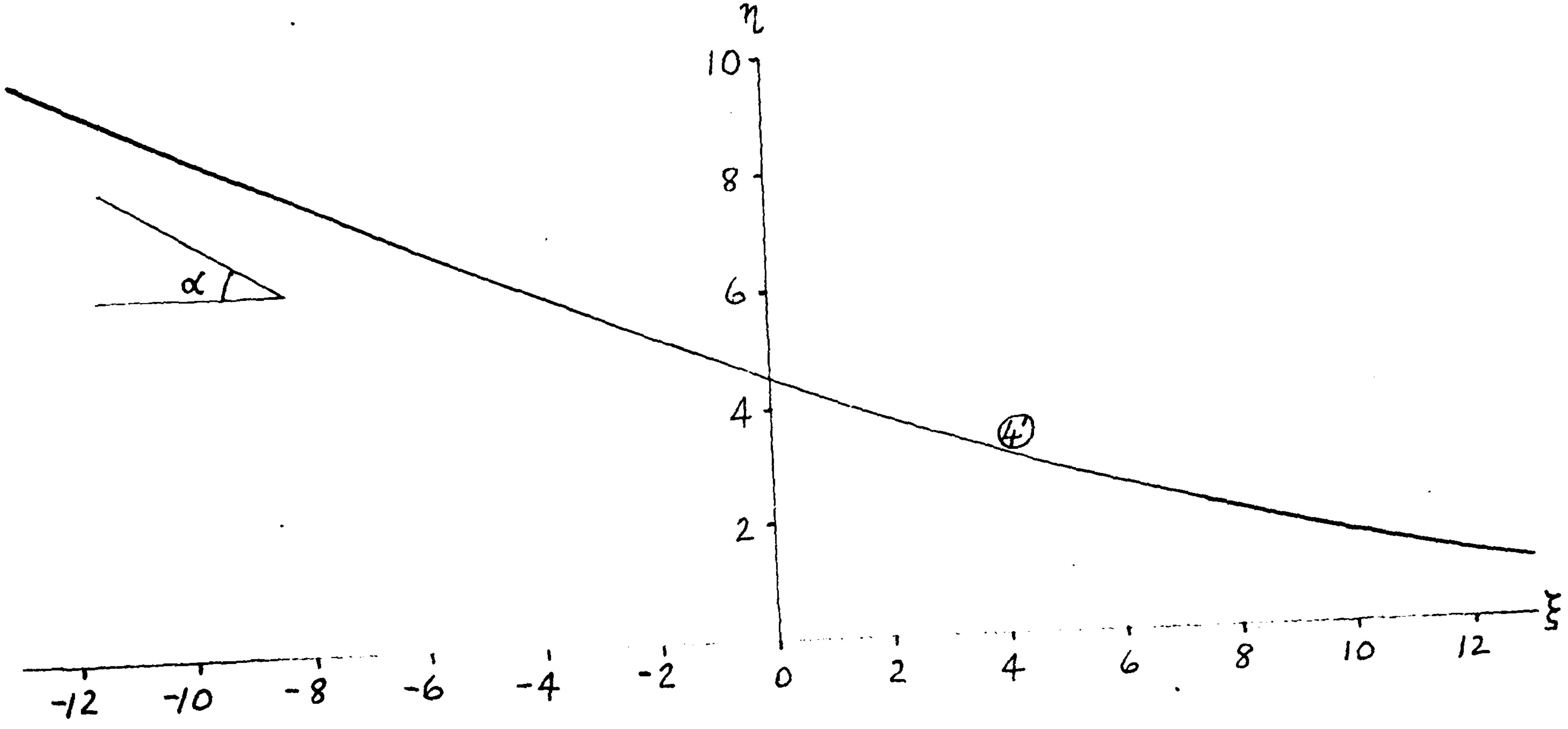

(c) Possible shapes for $\mathcal{L}<1$ $(k<0)$.

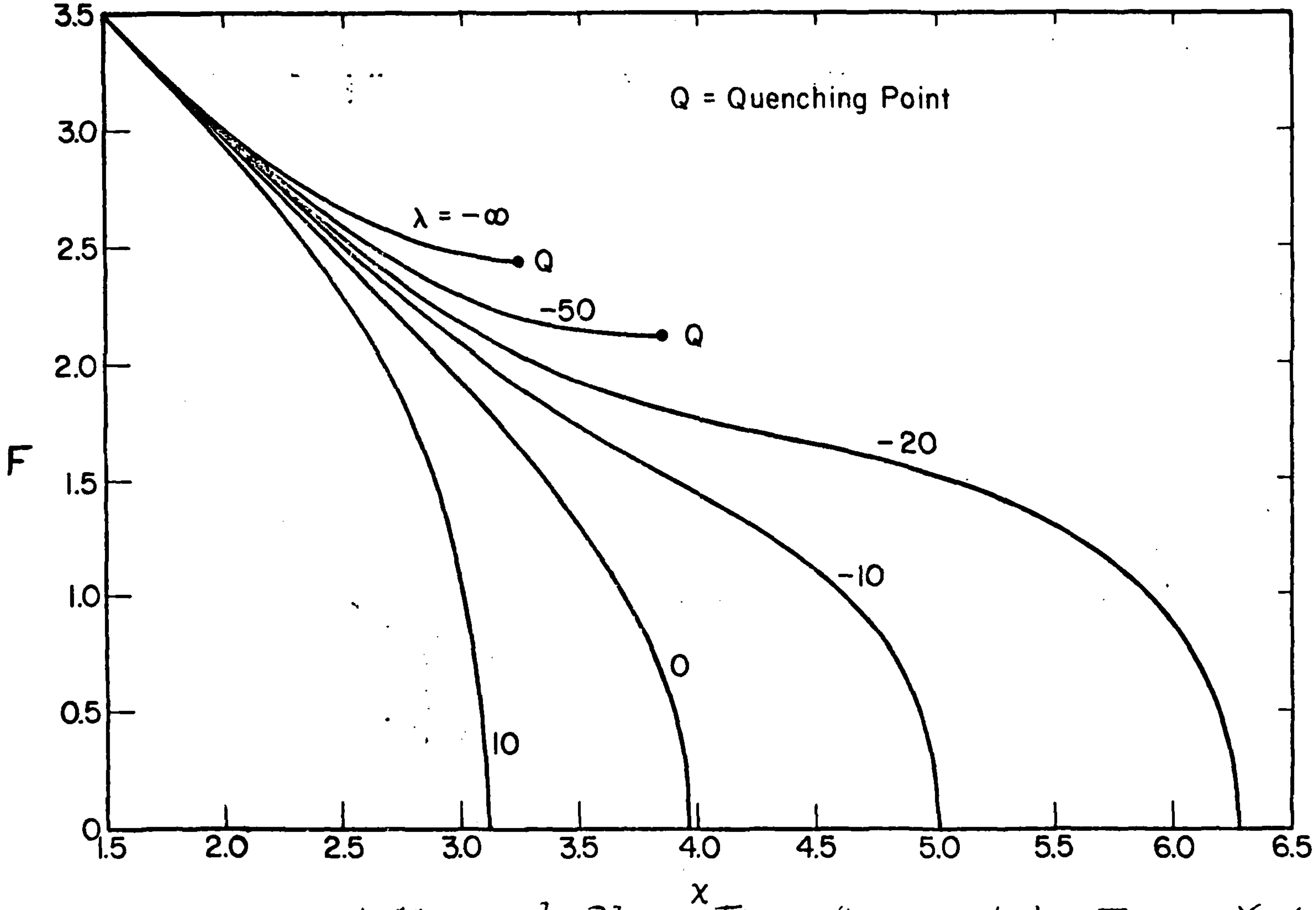

Fig. 6 Near-Equidiffusional Plane Tips. Computed for $T_1 = 0.2$, $Y_1 = 1$.

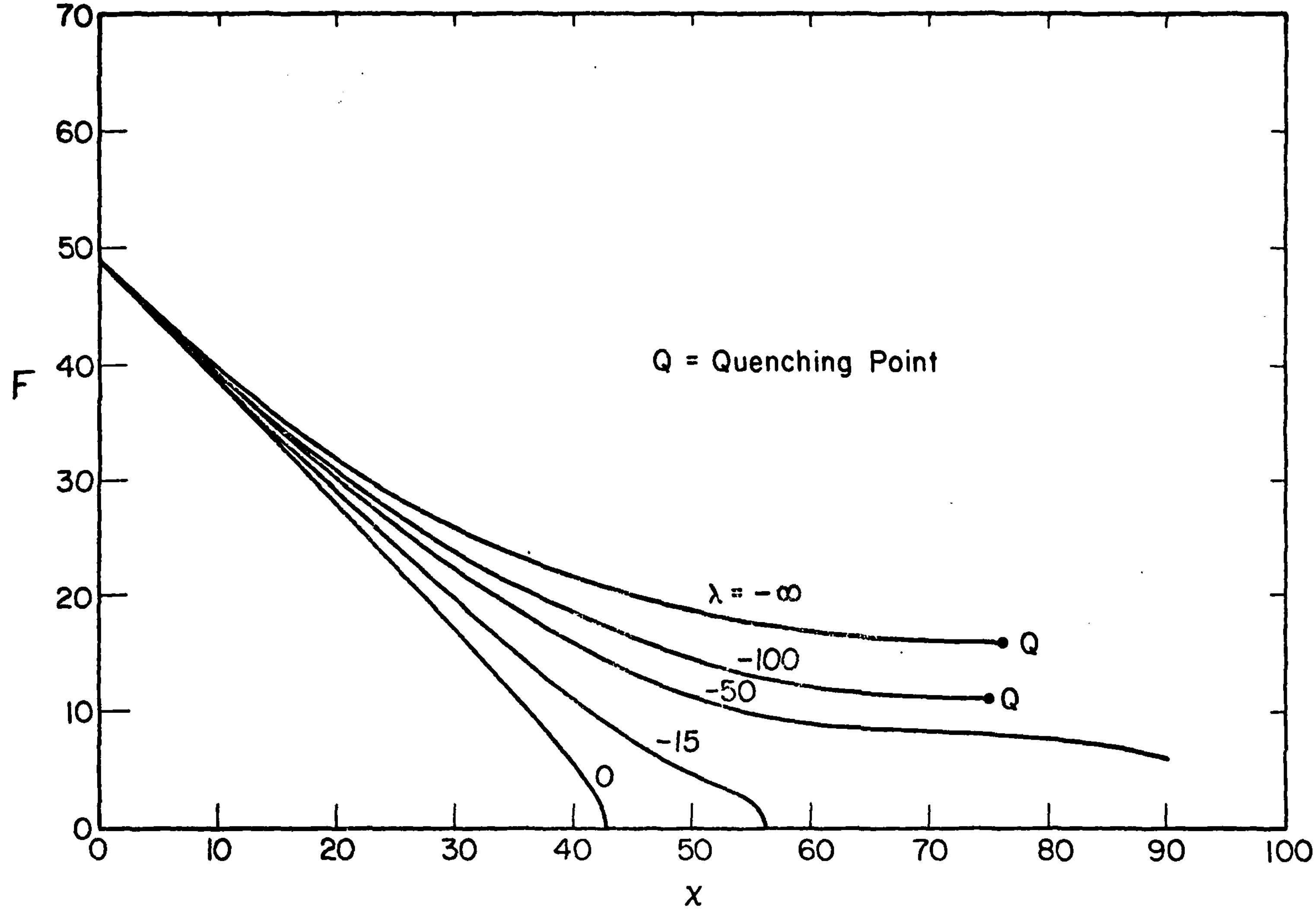

Fig. 7 Near-Equidiffusional Axisymmetric Tips Computed for same parameter values as Fig 6.

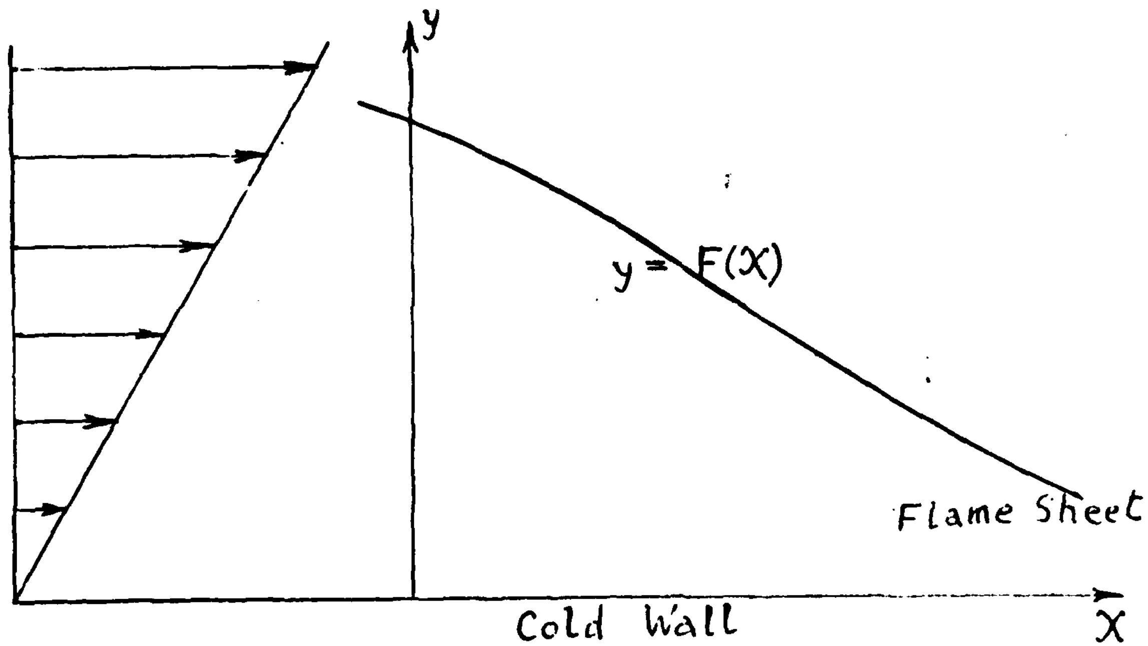

Fig. 8 Effect of cold wall on flame.

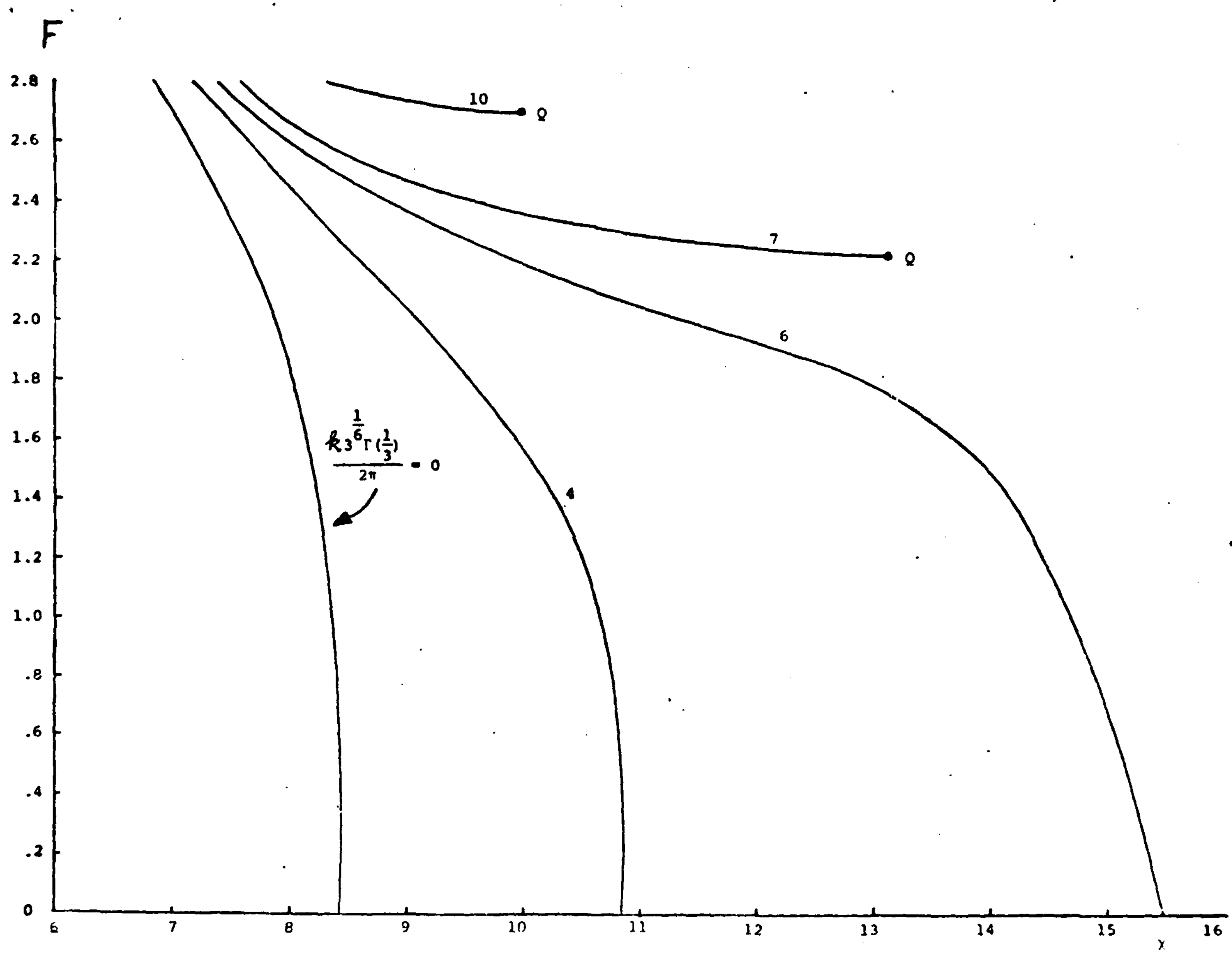

Fig. 9 Flame-sheet profiles for Fig 8, computed for $T_1 = 0.2$, $Y_1 = 1$.

SECURITY CLASSIFICATION OF THIS PAGE (When Data Entered)

REPORT DOCUMENTATION PAGE		READ INSTRUCTIONS BEFORE COMPLETING FORM
1. REPORT NUMBER 111	2. GOVT ACCESSION NO. AD-A083 547	3. RECIPIENT'S CATALOG NUMBER
4. TITLE (and Subtitle) MATHEMATICAL THEORY OF LAMINAR COMBUSTION IX: Burner Flames		5. TYPE OF REPORT & PERIOD COVERED Interim Technical Report
		6. PERFORMING ORG. REPORT NUMBER
7. AUTHOR(s) J.D. Buckmaster & G.S.S. Ludford		8. CONTRACT OR GRANT NUMBER(s) DAAG29-79-C-0121
9. PERFORMING ORGANIZATION NAME AND ADDRESS Dept. of Theoretical and Applied Mechanics Cornell University, Ithaca, NY 14853		10. PROGRAM ELEMENT, PROJECT, TASK AREA & WORK UNIT NUMBERS P-15882-M
11. CONTROLLING OFFICE NAME AND ADDRESS U. S. Army Research Office Post Office Box 12211 Research Triangle Park, NC 27709		12. REPORT DATE March, 1980
		13. NUMBER OF PAGES 31
14. MONITORING AGENCY NAME & ADDRESS (if different from Controlling Office)		15. SECURITY CLASS. (of this report) Unclassified
		15a. DECLASSIFICATION/DOWNGRADING SCHEDULE NA

16. DISTRIBUTION STATEMENT (of this Report)

Approved for public release; distribution unlimited.

17. DISTRIBUTION STATEMENT (of the abstract entered in Block 20, if different from Report)

NA

18. SUPPLEMENTARY NOTES

The findings in this report are not to be construed as an official Department of the Army position, unless so designated by other authorized documents.

19. KEY WORDS (Continue on reverse side if necessary and identify by block number)

Burner flames, anchored, hydrodynamics, tips, quenching, slowly varying, near-equidiffusional.

20. ABSTRACT (Continue on reverse side if necessary and identify by block number)

This report is Chapter IX of the twelve in a forthcoming research monograph on the mathematical theory of laminar combustion. The three parts of a burner flame (namely base, cone and tip) are examined using both the slowly varying and near-equidiffusional theories of Chapter VIII.